

## Effects of Disorder on the Collective Excitations in Helium

R. M. Dimeo,<sup>1</sup> P. E. Sokol,<sup>1</sup> D. W. Brown,<sup>1</sup> C. R. Anderson,<sup>2</sup> W. G. Stirling,<sup>2</sup> M. A. Adams,<sup>3</sup> S. H. Lee,<sup>4</sup>  
C. Rutiser,<sup>5</sup> and S. Komarneni<sup>5</sup>

<sup>1</sup>*Department of Physics, The Pennsylvania State University, University Park, Pennsylvania 16802*

<sup>2</sup>*Department of Physics, University of Liverpool, Liverpool, L697ZE, United Kingdom*

<sup>3</sup>*ISIS Facility, Rutherford Appleton Laboratory, Chilton, Didcot, Oxon. OX11 0QX, United Kingdom*

<sup>4</sup>*NIST, Gaithersburg, Maryland 20899*

<sup>5</sup>*Materials Research Laboratory, The Pennsylvania State University, University Park, Pennsylvania 16802*

(Received 14 July 1997)

We present inelastic neutron scattering measurements of the roton excitation of superfluid helium confined in two different porosity aerogels. The temperature dependence of the roton energy exhibits an anomalous crossover behavior at  $T_c = 1.9$  K. Below  $T_c$  the roton energy is found to be weakly temperature dependent while above  $T_c$  it varies more rapidly than the bulk. A simple qualitative model for this behavior in terms of a confined length scale is discussed. [S0031-9007(97)04946-6]

PACS numbers: 67.40.Hf, 61.12.Ex, 61.43.Gt

Liquid helium provides a model system on which the effects of disorder on superfluidity [1,2] and even high  $T_c$  superconductivity [3] have been studied. In high  $T_c$  superconductors it has been shown that dissipative superflow due to weakly pinned vortices is analogous to the dissipative superflow of helium in porous vycor glass [3]. The way in which disorder affects the macroscopic properties of liquid  $^4\text{He}$  has been investigated in detail. For example, the superfluid fraction, which is the fraction of the liquid that flows without viscosity, has been measured for several different types of confining media such as vycor, aerogel, and sol-gel glasses [4]. In vycor, which has a compact structure with well defined ( $\sim 70$  Å) pores and a single characteristic length scale, the superfluid transition is considerably suppressed but has the same critical exponent (0.674) as the bulk superfluid indicating that it remains in the same universality class [1,2]. In contrast, confinement in aerogel, which is formed by a gelation of a silica solution and is characterized by a wide range of length scales, changes the superfluid transition temperature by only a few millikelvin while drastically changing the critical exponent (0.813), indicating that the system is in a new universality class [1,5].

While the macroscopic effects of disorder have been extensively studied and a detailed understanding is developing there has been little work, either theoretical or experimental, on how disorder affects the collective excitations of the superfluid. For superfluid helium the collective excitations of importance are the phonon, which represents long wavelength density fluctuations (cf. sound waves in a solid), and the roton, which has historically been viewed as a microscopic vortex ring with a core just large enough for a single atom to pass through [6]. More modern theories treat the roton as a low energy, short wavelength density excitation, characteristic of the superfluid phase, with a wavelength characteristic of the interatomic spacing of the liquid [7]. These excitations

describe the microscopic dynamics of the superfluid and determine the macroscopic properties exhibited by the liquid. For example, the superfluid fraction and heat capacity, which are macroscopic properties, can be accurately obtained from the microscopic excitations by modeling the liquid as a noninteracting gas of phonons and rotons [8] except close to  $T_\lambda$  where the number density of rotons is very high. Although these excitations can be treated independently to yield the superfluid thermodynamics they are, in fact, part of the same dispersion curve as shown in Fig. 1 [9].

Measurements of the excitation spectrum of the liquid confined in aerogel at low temperatures ( $T < 1.3$  K) have shown that the excitations behave like those of the bulk liquid [8,10,11]. However, the temperature dependence of

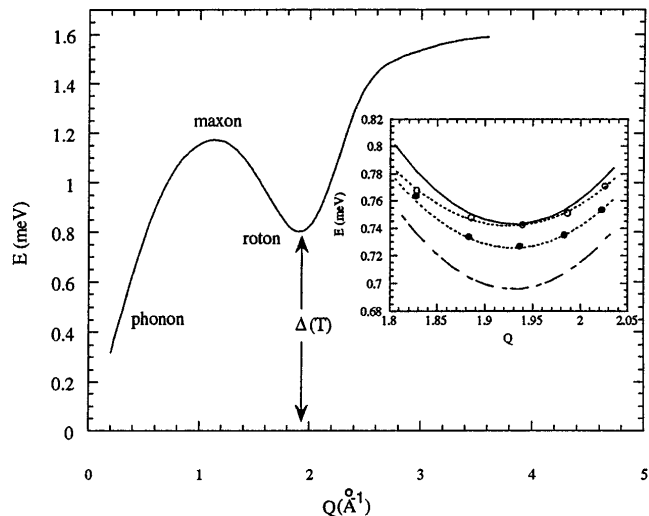


FIG. 1. Dispersion relation for superfluid helium. Inset: Roton minimum for bulk helium at 1.3 K (solid line) and 1.9 K (dash-dotted line) and the confined liquid at 1.3 K (open circles) and 1.96 K (solid circles). Dotted lines join the data points for the confined liquid.

the roton energy below 1.9 K is smaller than that observed in the bulk liquid. Sokol *et al.* have shown that this different temperature dependence can be directly related to the effective superfluid fraction of the confined liquid [8].

In this Letter we present new high resolution measurements of the collective excitations as determined by inelastic neutron scattering in the superfluid phase. Our measurements, which were carried out on samples of two different porosities, extend from 1.25 K, where previous measurements have shown that the collective excitations have the same energy as in the bulk liquid, to temperatures near the superfluid transition. These measurements show that there is a sharp crossover at approximately 1.9 K from a temperature variation that is weaker than the bulk for low temperatures to one that is stronger than the bulk at high temperatures. We present a simple model that identifies this crossover with a competition between the intrinsic length scale in the superfluid, which is set by the roton-roton interactions, and the length scale imposed by the confining medium.

We have performed inelastic neutron scattering measurements on superfluid helium in aerogels of 90% and 95% porosity. The measurements were carried out on the IRIS inverse time-of-flight spectrometer [12] at the ISIS pulsed neutron source (Rutherford Appleton Laboratory) and the SPINS triple-axis spectrometer (TAS) at the Cold Neutron Research Facility (CNRF), NIST. Using the pyrolytic graphite [002] analyzer reflection with a fixed final energy of 1.859 meV and an (elastic) energy resolution of 15  $\mu\text{eV}$ , the IRIS spectrometer covers a momentum transfer range of  $0.3 < Q < 2.1 \text{ \AA}^{-1}$  with an associated energy-transfer range of  $-0.2$  to 1.6 meV (neutron energy loss), spanning the phonon-maxon-roton region of the  $^4\text{He}$  dispersion curve. SPINS was operated in the constant  $Q$  mode with a fixed final analyzer energy of 2.6 meV producing an (elastic) energy resolution of 30  $\mu\text{eV}$ . In all measurements the temperature was measured by a germanium resistance thermometer with a stability of  $\pm 0.015$  K and the aerogel samples were filled to 95% full pore capacity with high purity  $^4\text{He}$  liquid. The neutron data were converted to the dynamic scattering function  $S(Q, E)$  using standard techniques [13,14]. The dynamic scattering function is directly proportional to the space and time Fourier transform of the density-density correlation function and provides direct information on the relative motions of the collective excitations which determine the properties of the liquid.

The dynamic scattering function of the  $^4\text{He}$  confined in aerogel is quite similar to that observed for bulk  $^4\text{He}$ , as reported previously [15]. The scattering function exhibits the familiar phonon-maxon-roton dispersion relation for the elementary excitations which are characteristic of  $^4\text{He}$  in the superfluid phase [15]. The single phonon-roton excitations are well defined and, after correcting for the finite instrumental resolution, could be least-squares fitted

to a single damped harmonic oscillator (DHO) form [16] (see Fig. 2). The DHO, which provides an excellent description of bulk  $^4\text{He}$  data, was used to obtain the roton energy and width (inverse lifetime).

In addition to instrumental resolution, the data were corrected for multiple scattering effects using standard correction techniques for neutron scattering from this system [15]. The excitation energies in the vicinity of the roton minimum are well described by the Landau expression [17]

$$E(Q, T) = \Delta(T) + \frac{\hbar^2(Q - Q_R)^2}{2\mu}, \quad (1)$$

as shown in the inset of Fig. 1, where  $\hbar Q_R$  is the roton momentum,  $\mu$  is the roton effective mass, and  $\Delta$  is the roton energy gap.

The temperature dependence of the roton energy gap,  $\Delta(T)$  for both the confined liquid and the bulk liquid, is shown in Fig. 3. At the lowest temperature studied  $\Delta(T)$  in the confined liquid is nearly identical to that of the bulk liquid. The variation with temperature, however, is quite different from that of the bulk. At low temperatures  $\Delta(T)$  in the confined liquid varies more slowly with temperature than in the bulk while at high temperatures  $\Delta(T)$  exhibits a stronger temperature dependence than the bulk. A sharp crossover between these two behaviors occurs at 1.9 K. This behavior is in distinct contrast to the behavior of the roton in bulk helium which is a smooth monotonically decreasing function of temperature as also can be seen in the figure. The experimental line shapes of Fig. 2 confirm these conclusions.

While detailed theories are still being developed, it is generally agreed that temperature variation of the roton

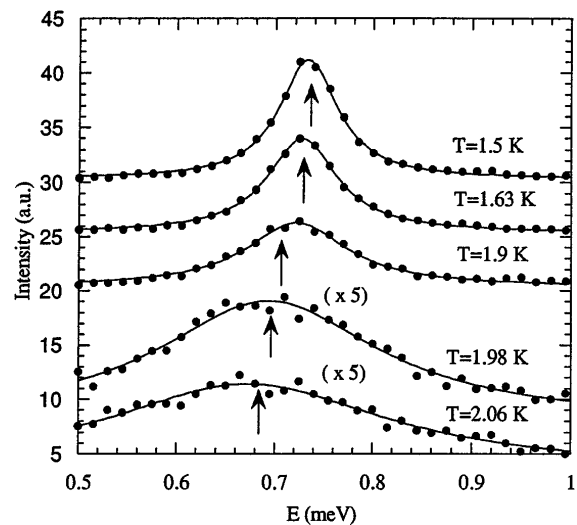


FIG. 2. Resolution-broadened scattering data (helium in 90% aerogel; IRIS) as a function of temperature at  $Q = 1.92 \text{ \AA}^{-1}$ . The arrows indicate the locations of the roton energy in the bulk liquid at each temperature [24]. The solid lines are DHO fits to the raw data.

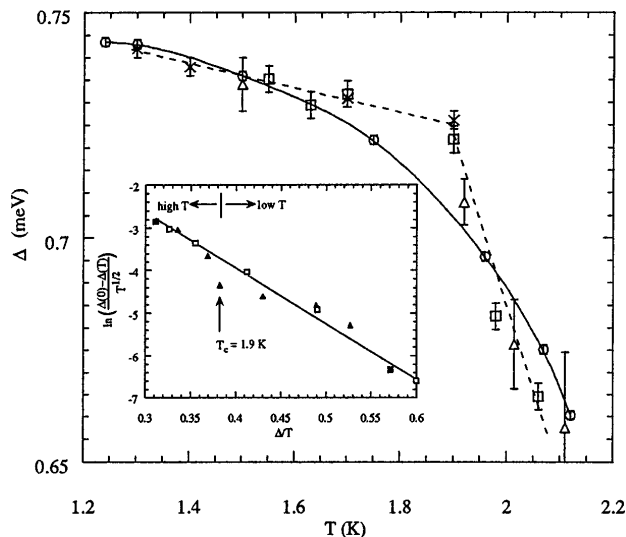


FIG. 3. Roton energy gap as a function of temperature. Open circles, bulk  $^4\text{He}$  data [24]; crosses,  $^4\text{He}$  in 95% aerogel [15]; open triangles, this work 95% aerogel (SPINS); open squares, this work 90% aerogel (IRIS). Smoothed dashed lines joining the points have been added as a guide to the eye. A distinct crossover behavior can be seen at 1.9 K. The inset shows data for the bulk (open squares) and confined liquid (95%—solid triangles) plotted in a manner suggestive of the mean free path for roton-roton interactions. The straight solid line is a fit to the bulk data. The confined liquid shows a clear departure from the bulk liquid which is most apparent at the crossover temperature.

energy gap and the linewidth in the bulk liquid arises from roton-roton interactions. Roton-roton scattering can be characterized by the roton mean free path  $l = \frac{1}{\sqrt{2n\sigma}}$  [18], where  $n$  is the number density of rotons and  $\sigma$  is the roton-roton scattering cross section. The interaction between rotons can be described in terms of an effective potential that is weakly attractive and gives a scattering cross section of  $\sim 7 \text{ \AA}^2$  [19]. The rotons may be treated as distinguishable particles as long as their density is low enough (i.e.,  $n_R \ll (\frac{Q_R}{2\pi})^3$ ). For low roton densities this results in a roton number density [20] of

$$n_R = \frac{2Q_R^2}{\hbar} \left( \frac{\mu k_B T}{8\pi^3} \right)^{1/2} e^{-\Delta/k_B T}. \quad (2)$$

This leads to a mean free path,  $l_R(T)$ , which is proportional to  $T^{-1/2} e^{\frac{\Delta}{k_B T}}$ . The roton energy for the bulk, shown in the inset in Fig. 3, is in good agreement with this predicted behavior. However, the energy of the confined liquid deviates from the behavior predicted for bulk liquid (straight line in inset of Fig. 3). This deviation is most pronounced at the crossover temperature.

The temperature dependence of the roton energy gap in the liquid confined in aerogel can be understood, qualitatively, in terms of a confinement length scale. The bulk liquid can be characterized by a temperature-dependent length scale—the roton mean free path  $l_R(T)$

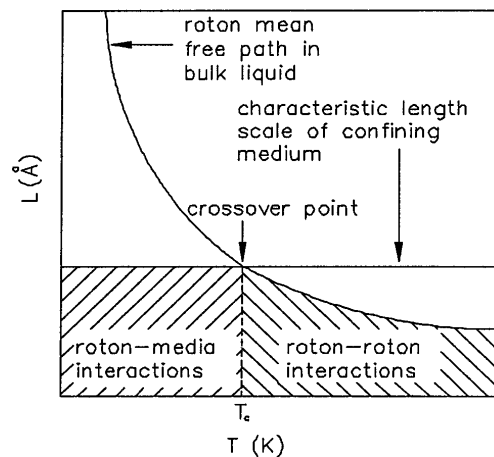


FIG. 4. Schematic representation of the two competing processes contributing to the crossover behavior in the roton energy. Roton-roton interactions have a strong temperature dependence yielding a strongly temperature-dependent mean free path whereas the roton-media interactions are approximately temperature independent. The intersection of the two curves separates the low temperature (weakly temperature-dependent) behavior from the higher temperature (strongly temperature-dependent) behavior.

which is illustrated in Fig. 4. For bulk helium it is *this* length scale which determines the temperature variation of the roton energy. Confinement in aerogel introduces a second length scale  $l_M$ , which is determined by elastic scattering of rotons from the fixed confining medium. This length scale will be set by the size of the open volume in the confining medium and the strength of the roton scattering. Since the pore size does not change with temperature, this second characteristic length scale will be a constant independent of temperature (see Fig. 4). At low temperatures the roton mean free path is much larger than  $l_M$  and the energy of the roton will be determined primarily by roton-medium scattering. At high temperatures  $l_R$  is less than  $l_M$  and roton-roton interactions will dominate the temperature dependence of the roton giving a behavior more similar to the bulk liquid. A crossover between these two different regimes will occur when  $l_M \sim l_R$ . The data above 1.9 K indicate that the temperature dependence of the roton energy is roughly the same as for the bulk but the values differ. This could be due to interactions between the rotons and thermally activated excitations. As one approaches  $T_\lambda$ , the interpretation of the temperature dependence is not easily addressed and becomes especially difficult in light of confinement. However, the simple model of Fig. 4 qualitatively describes the behavior of  $\Delta(T)$  for temperatures not too close to  $T_\lambda$ .

The density of rotons at this temperature,  $n_R(1.9 \text{ K})$ , is approximately  $1 \times 10^{-3}$  rotons/ $\text{\AA}^3$  giving a roton mean free path of  $\sim 100 \text{ \AA}$  in the bulk. Aerogel has an open interconnected pore structure with many silica strands

which can act as scattering centers. For a 90% porosity aerogel the silica strands are about 20–50 Å in diameter and each are separated roughly by 400 Å. The mean free path of a roton in this system ( $l = \frac{1}{n\sigma}$ ) is  $\sim 4500$  Å. This implies that the effect of the rotons interacting with the silica strands is negligible compared to the roton-roton interactions.

An alternative mechanism which can change the temperature dependence of the roton energy is trapped vorticity in the disordered geometry. It is known that rotons can interact with quantized vortex lines as well as with other rotons [7]. Trapped vortex lines pinned in the porous media could also give rise to a media induced scattering. Recent theories of the superfluid transition indicate that the appearance of thermally activated vortex lines plays a major role in the superfluid transition [21]. Using the areal line density [22],  $\sigma \sim 2 \ln(D/a_0)/D^2$  with a length scale due to confinement in the aerogel  $D \sim 400$  Å, a vortex core size of order  $a_0 \sim 1$  Å [23], and the roton-vortex line scattering length  $L_{RV} \sim 150$  Å [7] one finds the characteristic length scale  $d \sim 1/\sigma L_{RV}$  to be  $\sim 100$  Å which is of the same order as  $l_R$  at the crossover temperature. Thus the observed behavior of the roton may be due to roton-vortex scattering at low  $T$  and roton-roton scattering at high  $T$ .

The model of roton-vortex line scattering predicts that there should be a shift in the crossover temperature for confinement in materials of two different porosities. However, it is clear from Fig. 3 that no such difference is observable. One of the underlying assumptions of the roton-vortex scattering model is that the pore size distributions are narrow but aerogel, with its wide distribution of pore sizes, certainly does not fall into this category. Thus we expect that differences in the roton energy corresponding to differences in porosity on the order of 5% will be negligible. A rough estimate of the shift in the crossover temperature due to confinement in two materials with a narrow pore-size distribution with porosities of 90% and 95% is about 70 mK which may be observable. It is clear that future measurements should be carried out on helium confined to systems with narrow, well-defined pore-size distributions to confirm the relevance of the model we have applied here.

In summary, the roton excitation has been studied for superfluid helium in two different porosities of aerogel. For both samples, the roton energy exhibited a crossover behavior in temperature which can be attributed to the disorder introduced by confinement. This behavior can be interpreted in terms of length scales due to both confinement and the roton mean free path. While the roton mean free path sets the scale for temperatures above the crossover temperature, at temperatures below the crossover temperature the temperature dependence of the roton energy is suppressed. The effects of trapped vorticity are consistent with the observed behavior but it

is apparent that much more experimental work must be done to fully explore this possibility.

We wish to acknowledge the support of the National Science Foundation (9624762, INT 92-14242, and 9600172) and of the U.K. Engineering and Physical Sciences Research Council. We are grateful to the staff of ISIS and the CNRF for their assistance. The work on SPINS is based upon activities supported by the National Science Foundation under Agreement No. DMR-9423101. We also would like to thank Dr. Paul Chaikin for useful discussions.

- 
- [1] M. H. W. Chan, K. I. Blum, S. Q. Murphy, G. K. S. Wong, and J. D. Reppy, *Phys. Rev. Lett.* **61**, 1950 (1988).
  - [2] J. E. Berthold, D. J. Bishop, and J. D. Reppy, *Phys. Rev. Lett.* **39**, 348 (1977).
  - [3] A. Tyler, H. A. Cho, and J. D. Reppy, *Phys. Rev. Lett.* **73**, 987 (1994).
  - [4] P. A. Crowell *et al.*, *Phys. Rev. B* **51**, 12 721 (1995).
  - [5] G. K. S. Wong, P. A. Crowell, H. A. Cho, and J. D. Reppy, *Phys. Rev. B* **48**, 3858 (1993).
  - [6] R. P. Feynman and M. Cohen, *Phys. Rev.* **102**, 1189 (1956).
  - [7] R. J. Donnelly, *Phys. World* **10**, 25 (1997).
  - [8] P. E. Sokol, M. R. Gibbs, W. G. Stirling, R. T. Azuah, and M. A. Adams, *Nature (London)* **379**, 616 (1996).
  - [9] R. A. Cowley and A. D. B. Woods, *Can. J. Phys.* **49**, 177 (1971).
  - [10] J. De Kinder, G. Coddens, and R. Millet, *Z. Phys. B* **95**, 511 (1994).
  - [11] G. Coddens, J. De Kinder, and R. Millet, *J. Non-Cryst. Solids* **188**, 41 (1995).
  - [12] C. J. Carlile and M. A. Adams, *Physica (Amsterdam)* **182B**, 431 (1992).
  - [13] D. L. Price and K. Skold, *Methods of Experimental Physics*, edited by K. Skold and D. L. Price (Academic Press, New York, 1986), p. 1.
  - [14] RAL Report No. RAL-94-102 (1995).
  - [15] M. R. Gibbs, P. E. Sokol, W. G. Stirling, R. T. Azuah, and M. A. Adams, *J. Low Temp. Phys.* **107**, 33 (1997).
  - [16] W. G. Stirling and H. R. Glyde, *Phys. Rev. B* **41**, 4224 (1990).
  - [17] J. Wilks and D. S. Betts, *An Introduction to Liquid Helium* (Clarendon Press, Oxford, 1987).
  - [18] R. Kubo, *Statistical Mechanics: An Advanced Course with Problems and Solutions* (Elsevier Science Publishers, Amsterdam, 1965).
  - [19] P. H. Roberts and R. J. Donnelly, *J. Low Temp. Phys.* **15**, 1 (1974).
  - [20] J. Wilks, *The Properties of Liquid and Solid Helium*, (Clarendon Press, Oxford, 1967).
  - [21] G. A. Williams, *J. Low Temp. Phys.* **89**, 91 (1993).
  - [22] D. D. A. Awschalom and K. W. Schwarz, *Phys. Rev. Lett.* **52**, 49 (1984).
  - [23] G. W. Rayfield and F. Reif, *Phys. Rev.* **136**, A1194 (1964).
  - [24] K. H. Andersen and W. G. Stirling, *J. Phys. Condens. Matter* **6**, 5805 (1994).